Brownian Dynamics Simulations of Diffusional Encounters between Triose Phosphate Isomerase and Glyceraldhyde Phosphate: Electrostatic Steering of Glyceraldehyde Phosphate

ARTICLE *in* THE JOURNAL OF PHYSICAL CHEMISTRY · JANUARY 1993

Impact Factor: 2.78 · DOI: 10.1021/j100103a040

Brownian Dynamics Simulations of Diffusional Encounters between Triose Phosphate Isomerase and Glyceraldehyde Phosphate: Electrostatic Steering of Glyceraldehyde Phosphate

Brock A. Luty,* Rebecca C. Wade,† Jeffry D. Madura,‡ Malcolm E. Davis,§ James M. Briggs, and J. Andrew McCammon

Department of Chemsitry, University of Houston, Houston, Texas 77204-5641

Received: July 23, 1992; In Final Form: October 9, 1992

Brownian dynamics simulations of the diffusional encounter between the glycolytic enzyme triose phosphate isomerase (TIM) and its substrate, D-glyceraldehyde phosphate (GAP), were performed. GAP was modeled hydrodynamically as two touching spheres (a "dumbbell") using charges which reproduced the molecular dipole moment of the glyceraldehyde phosphate molecule as estimated by an ab initio molecular orbital calculation. The crystal structure of TIM was used to construct a detailed topographical and electrostatic grid on which the diffusion of the dumbbell was numerically simulated. By determining the number of diffusional encounters which resulted in GAP descending into the active sites of TIM with the appropriate orientation, the diffusion-controlled rate constant for the reaction was estimated to be 1.7×10^8 M^{-1} s^{-1}. This is in reasonable agreement with the experimentally determined diffusion-controlled rate constant of 4.8×10^8 M^{-1} s^{-1}. By reversing the direction of the dipole moment on the GAP model, it was shown that the orientational steering of the substrate by electrostatic torques can significantly increase the reaction rate constant. This effect is in addition to the previously established translational steering of the charged substrate by electrostatic forces.

1. Introduction

Triose phosphate isomerase (TIM) is the glycolytic enzyme which catalyzes the interconversion of D-glyceraldehyde phosphate (GAP) and dihydroxyacetone phosphate. The structural and kinetic properties of TIM have been studied extensively.[1-7] Structurally, TIM is a dimeric enzyme that has the special feature of a flexible loop near each of the active sites. The loops are disordered and probably mobile in the native enzyme but fold down to cover the active site when the substrate is bound.[6] Kinetically, the rate-limiting step has been shown to be the diffusional encounter of GAP with TIM.[7] TIM has been termed a "perfect" enzyme because any further acceleration of the catalytic steps that follow the binding of the substrate would have no effect on the overall reaction rate under physiological conditions.[4]

In this paper, we extend our previous study of the Brownian dynamics simulations of the diffusional encounter of GAP with TIM.[8] In the preliminary work, the substrate, GAP, was treated as a single sphere with a hydrodynamic radius of 2.5 Å and a charge of −2 e. The results demonstrated that the substrate was electrostatically steered toward the active sites of the enzyme. The estimated diffusion-controlled rate constant was almost 5 times larger when the electrostatic interaction between TIM and GAP was included, compared to the value calculated if the electrostatic interactions were ignored.

In this study, we add detail to the model of the substrate. Hydrodynamically, GAP is treated as two 2.0-Å-radius spheres connected by a rigid bond of 4.0 Å (see Figure 1). Four different charge schemes for the glyceraldehyde phosphate dumbbell model are examined: (1) no charges on either subunit, (2) equal charges on both subunits, (3) charges on the subunits to reproduce the molecular dipole, and (4) charges on the subunits to reproduce the magnitude of the molecular dipole but reverse its direction. Differences in the diffusion-controlled rate constants calculated for these charge models provide an estimate of the contributions of translational and orientational steering to the diffusion of glyceraldehyde phosphate into the active sites of the enzyme.

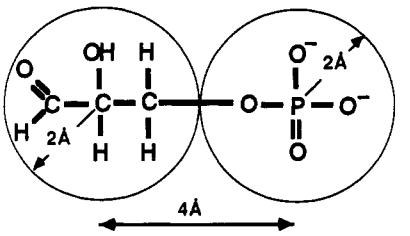

Figure 1. Schematic diagram of glyceraldehyde phosphate with the dumbell model superimposed. GAP is modeled as two touching spheres which represent the "glyceraldehyde" and "phosphate" moieties. The spheres are each assigned a central point charge and a hydrodynamic radius of 2.0 Å, which is approximately equal to the square root of the solvent-accessible surface area of each moiety divided by 4π. The spheres are connected by a rigid bond of 4.0 Å, which is approximately the distance between the center of geometry of the atoms of the two moieties.

In the next section, we describe the theory of Brownian dynamics simulations applied to a two-particle diffusing substrate. Section 3 describes the enzyme–substrate model used in the calculations. The results and a discussion are presented in section 4.

2. Theory

2.1. Brownian Dynamics. Brownian dynamics (BD) is a method that allows one to simulate the diffusional motion of a system of interacting solute particles. The method is based on a short time solution of the Langevin equation for a many body system.[9]

If we consider the center of the enzyme to be at the origin of a coordinate system, then the relative motion of a spherical subunit, i, of the substrate molecule may be simulated using

$$\mathbf{r}'_i = \mathbf{r}^0_i + \frac{\Delta t}{k_B T} \sum_{j=1}^{2} (\mathbf{D}_{ij} + \mathbf{D}_E) \cdot \mathbf{F}_j + \mathbf{S}_i \qquad (1)$$

where $\mathbf{r}^0_i$ and $\mathbf{r}'_i$ are the position vectors of substrate subunit i before and after a time step of Δt and $k_B T$ is Boltzmann's constant times the absolute temperature. In eq 1, hydrodynamic inter-

† Current address: European Molecular Biology Laboratory, Meyerhofstrasse 1, 6900, Heidelberg, Germany.

‡ Current address: Department of Chemistry, University of South Alabama, Mobile, AL 36688.

§ Current address: Macromolecular Modeling, Bristol-Myers Squibb Pharmaceutical Research Institute, P.O. Box 4000, Princeton, NJ 08543-4000.

0022-3654/58/2097-0233$04.00/0

actions between the subunits of the substrate are included, but those between the substrate and the enzyme are neglected. Because we are interested in an enzyme interacting with a much smaller substrate, the rotational diffusion of the enzyme is not important[10] and has been ignored in eq 1. The summation is over both substrate particles, $j = 1,2$. $\mathbf{F}_j$ is the force on substrate subunit j evaluated prior to the time step. $\mathbf{D}_{ij}$, with $i \neq j$, is the hydrodynamic interaction tensor between substrate subunits i and j evaluated prior to the time step; $\mathbf{D}_{ij}$, with $i = j$, is the diffusion constant of solute i multiplied by the identity tensor $\mathbf{I}$, and $\mathbf{D}_E$ is the diffusion constant of the enzyme multiplied by $\mathbf{I}$.

The diffusion constant for a spherical particle can be estimated using the Stokes–Einstein equation:

$$D = \frac{k_B T}{s\pi\eta a} \tag{2}$$

where a is the radius of the particle, η is the solvent viscosity, and s is equal to 6 (4) if stick (slip) boundary conditions are assumed for the surface of the particle.[11] Hydrodynamic interactions between the solute subunits can be approximated using a modified Oseen tensor:[12]

$$\mathbf{D}_{ij} = \frac{k_B T}{8\pi\eta r_{ij}}\left[\left(\mathbf{I} + \frac{\mathbf{r}_{ij}\mathbf{r}_{ij}^T}{r_{ij}^2}\right) + \frac{2a^2}{r_{ij}^2}\left(\frac{\mathbf{I}}{3} - \frac{\mathbf{r}_{ij}\mathbf{r}_{ij}^T}{r_{ij}^2}\right)\right] \tag{3}$$

where $\mathbf{r}_{ij}$ is the vector between solute sobunits i and j and the vector transpose is denoted by a superscript T. The inclusion of hydrodynamic interaction between the subunits is necessary to produce the translational and rotational motion expected for the dumbbell model of the substrate.

The $\mathbf{S}_i$ are vectors of Gaussian random numbers which have zero mean and variance–covariance:

$$\langle \mathbf{S}_i \mathbf{S}_j^T \rangle = 2(\mathbf{D}_{ij} + \mathbf{D}_E)\Delta t \tag{4}$$

The $\mathbf{S}_i$ represent stochastic displacements of the solute particle due to random collisions with the solvent and satisfy the fluctuation–dissipation theorem.

The geometry (i.e., the bond length) of the dumbbell can be maintained by two techniques: (1) an intersubunit restraining force can be included in 1, or (2) an unconstrained step made with eq 1 may be followed by a correction step in which the constraints are satisfied exactly. Two methods of applying the latter technique, a method originally developed by Allison and McCammon,[13] shake-HI, and a variation which was used in this work, are described in Appendix A.

It should be noted that Allison et al.[14] have also studied the diffusional motion of a dumbell substrate. They, however, investigated the case of a spherical enzyme interacting with the substrate through a centrosymmetric potential.

2.2. Diffusion-Controlled Rate Constants. Brownian dynamics can be used to determine the rates of diffusional encounter through the relation[15-17]

$$k = k(b)\beta \tag{5}$$

where $k(b)$ is the rate at which the enzyme and the substrate would first reach a separation b and β is the combination probability from this distance. If the distance b is chosen to be sufficiently large so that the interparticle potential of mean force, $U(r)$, is approximately zero, then $k(b)$ is given by the Smoluchowski equation:[18]

$$k(b) = 4\pi D b \tag{6}$$

where D is the relative diffusion coefficient which is assumed to be constant for a separation distance greater than b.

The contribution of the detailed dynamics of the substrate near the enzyme to the rate of diffusional encounter is contained in the combination probability β. β is determined by running a number of trajectories in which the enzyme and the substrate are initially separated by a distance b at a random relative orientation and diffusion is simulated numerically (e.g., using eq 1) until (1) the substrate reaches the active site and satisfies a set of reaction criteria (see next section) or (2) the substrate diffuses to a separation m ($>b$). If the substrate reaches a distance m, then an analytic solution of the diffusion equation is used to determine the probability that the substrate would diffuse to an infinite separation or return to a separation b at which the numerical diffusion must be restarted.[19] Appendix B contains a description of this procedure. The quantity β is the ratio of the number of trajectories which satisfy the reaction criteria to the total number of trajectories.

3. Model System

The three-dimensional Cartesian coordinates for chicken muscle TIM were taken from the 1988 Brookhaven National Laboratory Protein Data Bank Tape (file 1TIM).[5] In the crystal structure, the two monomers of the TIM dimer do not have identical structures, differing most in the regions near the flexible loops. A symmetric TIM dimer was constructed by replacing subunit II of the dimer with a duplicate of subunit I which had been rotated and translated to overlay the atoms of the original subunit II. An investigation of the gating of the active site by the flexible loop has been performed.[20] The results of this investigation demonstrate that the gating period of the loop is short compared to the time scale of the substrate–enzyme diffusional motion, and therefore, the gating motion of the loops does not significantly affect the rate of reaction. To simplify the present calculation, the loops are held in the open, unperturbed conformation.

Hydrogen atoms were added to the polar atoms (N and O) using the CHARMm program.[21] All titrating residues were assigned their usual protonation state at neutral pH. Charges were assigned to all atoms using the OPLS parameter set.[22] The net charge on TIM was zero. The shape of the low dielectric region defined by the protein was determined by assigning each atom in TIM a standard radius for protein atoms.[23] This low dielectric volume along with the charges assigned to each atom was mapped onto a $(110)^3$ grid with 1.0-Å grid spacing.[24,25] An incomplete Cholesky conjugate gradient method was used to solve the finite-difference linearized Poisson–Boltzmann equation for the electrostatic potential at the grid points.[26] Dielectric constants for the regions interior and exterior to the protein were assigned values of 2 and 78, respectively, and the boundary between the regions was assigned intermediate values.[27] The region outside the protein had ions distributed according to Boltzmann weighting of the electrostatic potential. The bulk ionic strength was assigned a value of 0.1 M.

From preliminary electrostatic calculations, using a large grid spacing, it was estimated that the potential surrounding the enzyme was approximately zero (all potentials less than $\pm k_B T/4$) at a distance of 55 Å from the center of the enzyme. This value was chosen as the distance b, and the distance m was chosen as 75 Å. The diffusion constant of TIM, D_E, was calculated using eq 2 assuming stick boundary conditions ($s = 6$) and a hydrodynamic radius of 40 Å which corresponds to about half of the largest dimension of the enzyme. To increase the efficiency of the algorithm, a variable time step was used in eq 1 which was dependent on the distance of the substrate from the center of the enzyme. The time step was defined by the following function:

$$\Delta t = \begin{cases} 1.0 \text{ ps} & \text{if } r < 55 \text{ Å} \\ 5.0 \text{ ps} & \text{if } r > 55 \text{ Å} \end{cases} \tag{7}$$

These values are sufficiently small that, during a time step, (1) the change in force on the substrate is small, (2) the reflecting surface of the enzyme was represented to the accuracy of the grid, and (3) the translational and rotational diffusion constants of the dumbbell were approximately equal to the values that can be determined analytically (see Appendix A).

TABLE I: Calculated Diffusion-Controlled Rate Constant for the Reaction between Triose Phosphate Isomerase and Glyceraldehyde Phosphate for Different Sets of Reaction Criteria and Different Models of Glyceraldehyde Phosphate[a]

substrate model	charge glyc	charge phos	A (<8 Å)	B (<5 Å)	C (both <1 Å)
monomer	0.0		30.87 (1.30)	14.33 (0.90)	
	-1.0		57.12 (1.71)	38.75 (1.44)	
	-2.0		108.37 (2.19)	94.12 (2.09)	
dumbbell	0.00	0.00	30.39 (1.25)	13.18 (0.84)	0.062 (0.058)
	-0.50	-0.50	53.28 (1.61)	35.38 (1.34)	0.164 (0.096)
	-0.15	-0.85	54.99 (1.63)	36.67 (1.36)	0.062 (0.058)
	-0.85	-0.15			0.062 (0.058)
	-1.00	-1.00	95.62 (2.02)	80.94 (1.90)	0.534 (0.172)
	-0.30	-1.70	101.38 (2.06)	86.96 (1.95)	1.664 (0.303)
	-1.70	-0.30			0.144 (0.089)

[a] Values are in units of 10^8 M^{-1} s^{-1}. The experimentally determined value is 4.8×10^8 M^{-1} s^{-1}. Error estimates (90% confidence interval) are given in parentheses.

The pK_a of the monoanionic glyceraldehyde phosphate is approximately 6.75.[28] At pH 7.0, an unperturbed GAP molecule will be partitioned almost equally between the singly and doubly deprotonated states. The results for both species are included in this study.

Approximate molecular dipole moments for these two species were computed by first determining optimized geometries at the semiempirical level (MNDO) using Gaussian 90.[29] To obtain a better description of the electronic distribution, and hence a better estimate of the molecular dipole moment, single-point calculations were carried out with the STO-3G basis set (STO-3G//MNDO). The molecular dipole moments for the singly and doubly deprotonated glyceraldehyde phosphate were 7.36 and 13.44 D, respectively. For the dumbbell model, the appropriate charges to approximately reproduce the molecular dipole moments are -0.15 e on the "glyceraldehyde" subunit and -0.85 e on the "phosphate" subunit for the monoanion and -0.3 e on the "glyceraldehyde" subunit and -1.7 e on the "phosphate" subunit for the dianion.

Reaction criteria were established by docking an all atom model of GAP in the active site of TIM using the molecular graphics program Quanta from Molecular Simulations.[30] The atoms of the substrate were positioned in approximate agreement with coordinate information from cocrystallization of yeast TIM with the substrate analogue phosphoglycolate.[31] The dumbbell model of GAP was then superimposed on the all atom model to locate two points to be used in the definition of reaction criteria. The docked position of the dumbbell's glyceraldehyde subunit was chosen to be 8.8, 8.2, 6.6, 4.6, and 7.0 Å from the α carbons of residues His 94, Glu 164, Ser 210, Gly 231, and Gly 232, respectively. The docked position of the dumbbell's phosphate subunit was chosen to be 12.5, 10.7, 4.8, 4.9, and 5.2 Å from the α carbons of residues His 94, Glu 164, Ser 210, Gly 231, and Gly 232, respectively.

From these two defined points, two types of reaction criteria were constructed. A set of loose criteria was defined by requiring only one of the subunits of the substrate to come within a prescribed distance of the docked dumbbell's phosphate position. The docked dumbbell's phosphate moiety is positioned near the mouth of the active site channel, and these loose criteria define a "cap" over the active site. A set of tight criteria were defined by requiring the glyceraldehyde subunit of the substrate to approach within a prescribed distance of the docked dumbbell's glyceraldehyde position simultaneously with the phosphate subunit of the substrate coming within the same prescribed distance of the docked dumbbell's phosphate position.

A more detailed model of the enzyme would allow for the dynamics of the atoms in the active site. The thermal motion of these atoms would cause the "tunnel" to the active site to expand and contract in width. In our static model of the protein structure, this motion is not allowed and we chose to scale the atomic radii of the atoms in the active site to compensate for this deficiency. All the atomic radii of the residues which were within 3.5 Å of the docked all atom representation of the GAP molecule (Asn 10, Lys 12, His 94, Glu 164, Ala 168, Ile 169, Gly 170, Ser 210, Val 211, Gly 231, and Gly 232) were scaled by 0.66.

All the electrostatic and Brownian dynamics calculations described here were carried out with the UHBD program.[32]

4. Results and Discussion

The results of this study along with error estimates (90% confidence interval) are summarized in Table I. Also included for comparison are some new results for GAP modeled hydrodynamically as a single sphere (monomer). The two columns of Table I labeled A and B are for the loose criteria which only required either of the two subunits of the dumbbell (or the single unit of the monomer) to come within 8.0 Å (column A) or 5.0 Å (column B) of the docked dumbbell's phosphate position. The last column in Table I (column C) is for the tight criteria which required the glyceraldehyde subunit of the substrate to come within 1.0 Å of the docked dumbbell's glyceraldehyde position simultaneously with the phosphate subunit of the substrate coming within 1.0 Å of the docked dumbbell's phosphate position. The value of 1.0 Å was chosen as a balance between being large enough to minimize the importance of the arbitrarily selected positions of the reaction criteria and being small enough to correctly discriminate the orientation of the dumbbell. Twenty thousand trajectories were performed for each substrate model.

As determined in the previous study, the diffusion-controlled rate constant for the association of the monomer GAP model with the enzyme is dramatically increased by electrostatic steering. The rate constant for the singly charged species was increased 2-3-fold over the value determined when the electrostatic interactions between the substrate and the enzyme were ignored. The rate constant for the doubly charge species was increased by a factor of 3.5-6.6 by electrostatic steering, in agreement with our previous study.

For the "loose" criteria, the rate of association of the GAP dumbbell model is very similar to the values for the correspondingly charged monomer models. Note that the translational diffusion constant of the monomer model is approximately 6% higher than the diffusion constant for the dimer. On this basis, we would expect that the rate constant for the monomer model would be approximately 6% higher than the rate constants for the dimer model. The agreement between the results for the monomer and the dimer implies that the details of the substrate are not very important in regions outside the active site. However, for the doubly charged dumbbell model, there was a slight increase in the rate for reaching the loose criteria when the dumbbell had a dipole moment. This is also true for the singly charged dumbbell model with a dipole moment, but the enhancement of the rate, over the corresponding model without the dipole moment, is smaller than the estimated error in the results. Two factors may

be responsible for the small enhancement. First, if there is a gradient in an electric field, then the dumbbell model with a dipole will feel a net force that the model without the dipole will not feel, possibly leading to stronger steering of the substrate. Second, if the electric field is pointed in the direction of the active site, then a dipole on the dumbbell would tend to align with this field. The diffusion constant of the dumbell along the symmetry axis is approximately 12% higher than the diffusion constant for translation perpendicular to the axis. A dumbell which is aligned toward the active site could therefore have a larger chance of reaching the active site relative to a dumbbell which is always perpendicular to the active site. But, in total, this is still a small effect.

Because of the relatively low probability of the substrate satisfying the "tight" reaction criteria, the values in column C have a relatively larger error and are more difficult to interpret. The most interesting results are for the doubly charged species where having the correct dipole moment can increase the rate approximately 3-fold over the model without a dipole and 10-fold over the model with the dipole pointing in the wrong direction. This effect is due to the large electric fields in the active site which favor the correct orientation of the dumbell over the opposite orientation.

The experimental value for the diffusion-controlled rate constant is 4.8×10^8 M^{-1} s^{-1}.[3] This value is within a factor of 3 of the rate constant for the tight, orientationally specific, reaction criteria for the GAP model with a charge of −2 e and realistic dipole moment. Although the calculated rate is sensitive to the parameters used in this model, the calculations yield an important new conclusion: For a fairly realistic model of an enzyme and a polar substrate, orientational steering of the substrate by electrostatic torques can significantly increase reaction rate constants. This effect is in addition to the established translational steering of charged substrates by electrostatic forces.

Acknowledgment. This work was supported in part by the NIH, the Robert A. Welch Foundation, and the NCSA. B.A.L. is the recipient of an NIH Predoctoral Traineeship in the Houston Area Molecular Biophysics Program. J.A.M. is the recipient of the G.H. Hitchings Award from the Burroughs Wellcome Fund.

Appendix A: Applying Geometric Constraints

An unconstrained step of the subunits of the solute using eq 1 must be followed by a correction step to maintain the distance (bond length) between the subunits of the substrate. For a dumbbell, the constraining force operates between the two subunits, and the corrections $\delta\mathbf{r}_i$ can be written[13]

$$\delta\mathbf{r}_1 = g[\mathbf{D}_{12}-\mathbf{D}_{11}]\cdot\mathbf{r} \tag{8}$$

$$\delta\mathbf{r}_2 = g[\mathbf{D}_{22}-\mathbf{D}_{12}]\cdot\mathbf{r} \tag{9}$$

where g is unknown (the magnitude of the constraining force) and $\mathbf{r} \equiv \mathbf{r}_2 - \mathbf{r}_1$ is the vector between the subunits. Subtracting the first equation from the second, we find ($\delta\mathbf{r} \equiv \delta\mathbf{r}_2 - \delta\mathbf{r}_1$)

$$\delta\mathbf{r} = g\mathbf{D}\cdot\mathbf{r} \tag{10}$$

where $\mathbf{D} \equiv \mathbf{D}_{11} - 2\mathbf{D}_{12} + \mathbf{D}_{22}$.

If we evaluate eq 10 prior to the unconstrained step, then

$$\delta\mathbf{r} = g^0\mathbf{D}^0\cdot\mathbf{r}^0 = g^0\kappa\mathbf{r}^0 \tag{11}$$

where κ is calculated from $\kappa\mathbf{r}^0 = \mathbf{D}^0\cdot\mathbf{r}^0$ (see below). The value of g^0 can be determined using

$$\mathbf{r}^2 = d^2 = (\mathbf{r}' + \delta\mathbf{r})^2 \tag{12}$$

where d is the bond length and $\mathbf{r}'$ is the vector between the subunits after the unconstrained step. The result to first order in g^0 is[13]

$$g^0 = \frac{1}{2\kappa}\left(1 - \frac{(\mathbf{r}')^2}{d^2}\right) \tag{13}$$

If we evaluate eq 10 after the unconstrained step, then

$$\delta\mathbf{r} = g'\mathbf{D}'\cdot\mathbf{r}' = g'\kappa\mathbf{r}' \tag{14}$$

The value of g' can be determined using

$$\mathbf{r} = \mathbf{r}' + \delta\mathbf{r} = (1 + g'\kappa)\mathbf{r}' \tag{15}$$

The result is

$$g' = \frac{1}{\kappa}\left(\frac{d}{|\mathbf{r}'|} - 1\right) \tag{16}$$

As mentioned, the value of κ is determined by solving

$$\kappa\mathbf{r} = \mathbf{D}\cdot\mathbf{r} \tag{17}$$

where $\mathbf{D} \equiv \mathbf{D}_{11} - 2\mathbf{D}_{12} + \mathbf{D}_{22}$. To keep the following expressions general, we assume that the subunits are not necessarily of the same size (i.e., $a_1 \neq a_2$) and that they are not necessarily touching (i.e., $a_1 + a_2 \neq d$). For hydrodynamic interaction between nonequal-sized subunits, we use the modified Oseen tensor as generalized by Garcia de la Torre and Bloomfield:[33]

$$\mathbf{D}_{ij} = \frac{k_B T}{8\pi\eta r_{ij}}\left[\left(\mathbf{I} + \frac{\mathbf{r}_{ij}\mathbf{r}_{ij}^T}{r_{ij}^2}\right) + \frac{a_i^2 + a_j^2}{r_{ij}^2}\left(\frac{\mathbf{I}}{3} - \frac{\mathbf{r}_{ij}\mathbf{r}_{ij}^T}{r_{ij}^2}\right)\right] \tag{18}$$

The resulting correction equations are for the first method

$$\delta\mathbf{r}_1 = \frac{C_1}{C}\frac{1}{2}\left(1 - \frac{(\mathbf{r}')^2}{d^2}\right)\mathbf{r}^0 \tag{19}$$

$$\delta\mathbf{r}_2 = -\frac{C_2}{C}\frac{1}{2}\left(1 - \frac{(\mathbf{r}')^2}{d^2}\right)\mathbf{r}^0 \tag{20}$$

and for the second method

$$\delta\mathbf{r}_1 = \frac{C_1}{C}\left(\frac{d}{|\mathbf{r}'|} - 1\right)\mathbf{r}' \tag{21}$$

$$\delta\mathbf{r}_2 = -\frac{C_2}{C}\left(\frac{d}{|\mathbf{r}'|} - 1\right)\mathbf{r}' \tag{22}$$

where

$$C_1 = \frac{1}{sa_1} - \frac{1}{4d}\left(1 - \frac{a_1^2 + a_2^2}{3d^2}\right) \tag{23}$$

$$C_2 = \frac{1}{sa_2} - \frac{1}{4d}\left(1 - \frac{a_1^2 + a_2^2}{3d^2}\right) \tag{24}$$

$$C = C_1 + C_2 = \frac{1}{s}\left(\frac{1}{a_1} + \frac{1}{a_2}\right) - \frac{1}{2d}\left(1 - \frac{a_1^2 + a_2^2}{3d^2}\right) \tag{25}$$

For the situation of $a_1 = a_2$, the values of C_1/C and C_2/C are $^1/_2$ as expected.

Both methods of applying constraints were examined for the dumbbell model used in this work. For simulation time steps of less than 1 ps, it was found that both methods of constraint could reproduce the translational and rotational diffusion constants with less than 1% deviation from the values which can be determined analytically.[33] However, at the 1-ps time step, the method using eqs 19 and 20 required an average of 1.5 iterations, whereas the method using eqs 21 and 22 required only 1 iteration. Furthermore, eqs 19 and 20 were not able to satisfy the geometric

constraints at time steps larger than 5 ps. In contrast, the method using eqs 21 and 22 was able to reproduce the translational diffusion constant with less than 1% error, and the rotational diffusion constant with less than 10% error for time steps up to 10 ps.

Appendix B: Determination of Escape Probability from the M Surface

A substrate which reaches a distance m ($>b$) from the enzyme has two possible fates: (1) escape to an infinite separation or (2) diffuse back to a separation b. In the situation that the interaction potential is approximately zero at distances larger than b, the probability that the particle escapes to infinity is simply[19]

$$p_{\text{escape}} = 1 - \lambda \tag{26}$$

where $\lambda = b/m$.

To analyze the situation in which the substrate returns to a separation b, consider a spherical polar coordinate system with the origin at the center of the enzyme and the polar axis passing through the point at which the substrate reached a distance m. The probability distribution for the positions that the substrate will return to a separation b is symmetric about the polar axis (azimuthal symmetry) and can be determined analytically by solving the diffusion equation[19]

$$p(x) = \frac{\lambda}{2}\frac{1-\lambda^2}{(1-2\lambda x+\lambda^2)^{3/2}} \tag{27}$$

where x is the cosine of the polar angle. To select an angle from this probability distribution, we first construct the cumulative distribution function (see, e.g., ref 34):

$$F(x) = \int_{-1}^{x} p(x)\,dx = \frac{1-\lambda^2}{2}\left[\frac{1}{(1-2\lambda x+\lambda^2)^{1/2}} - \frac{1}{1+\lambda}\right] \tag{28}$$

This expression is then inverted to find x as a function of $F(x)$:

$$x = \frac{1+\lambda^2}{2\lambda} - \frac{1}{2\lambda}\left[\frac{1-\lambda^2}{2F(x)+1-\lambda}\right]^2 \tag{29}$$

If a substrate reaches a distance m from the enzyme, a random number $\mathcal{R}$ is selected uniformly on [0,1]. If $\mathcal{R} > \lambda$, then the substrate escapes to infinity (i.e., the trajectory is terminated). If $\mathcal{R} < \lambda$, then the value is substituted into eq 29 (for $F(x)$), which yields the polar angle at which to resume numerical diffusion at a distance b.

For the dumbbell substrate, the difference between m and b is made sufficiently large that it can be assumed that the rotational orientation of the dimer would be fully relaxed on diffusing this distance. If this criterion is met, then the dumbbell orientation can be selected from a random distribution when the numerical diffusion is resumed at the distance b.

References and Notes

(1) Banner, D. W.; Bloomer, A. C.; Petsko, G. A.; Phillips, D. C.; Pagsoon, C. I.; Wilson, I. A. *Biochem. Soc. Trans.* **1976**, *72*, 146.
(2) Albery, J. R.; Knowles, W. J. *Biochemistry* **1976**, *15*, 5627.
(3) Phillips, D. C.; Rivers, P. S.; Sternberg, M. J. E.; Thorton, J. M.; Wilson, I. A. *Biochem. Soc. Trans.* **1977**, *5*, 642.
(4) Knowles, J. R.; Albery, W. J. *Acc. Chem. Res.* **1977**, *10*, 105–111.
(5) Banner, D. W.; Bloomer, A. C.; Petsko, G. A.; Phillips, D. C.; Pogsoon, C. I.; Wilson, I. A. *Nature (London)* **1981**, *255*, 609.
(6) Alber, T.; Gilbert, W. A.; Ponzi, D. R.; Petsko, G. A. Mobility and Function in Proteins and Nucleic Acids. In *Ciba Foundation Symposium 93*; Pitman: London, 1983.
(7) Blacklow, S. C.; Raines, R. T.; Lim, W. A.; Zamore, P. D.; Knowles, J. R. *Biochemistry* **1988**, *27*, 1158.
(8) Madura, J. D.; McCammon, J. A. *J. Phys. Chem.* **1989**, *93*, 7285–7287.
(9) Ermak, D. L.; McCammon, J. A. *J. Chem. Phys.* **1978**, *69*, 1352–1360.
(10) Shoup, D.; Lipari, G.; Szabo, A. *Biophys. J.* **1981**, *36*, 697–714.
(11) Doi, M.; Edwards, S. F. *The Theory of Polymer Dynamics*; Clarendon Press: Oxford, 1986.
(12) Rotne, J.; Prager, S. *J. Chem. Phys.* **1969**, *50*, 4831–4837.
(13) Allison, S. A.; McCammon, J. A. *Biopolymers* **1984**, *23*, 167–187.
(14) Allison, S. A.; Srinivasan, N.; McCammon, J. A.; Northrup, S. H. *J. Phys. Chem.* **1984**, *88*, 6152.
(15) Northrup, S. H.; Allison, S. A.; McCammon, J. A. *J. Chem. Phys.* **1984**, *80*, 1517–1524.
(16) Zhou, H.-X. *J. Chem. Phys.* **1990**, *92*, 3092–3095.
(17) Davis, M. E.; Madura, J. D.; Sines, J.; Luty, B. A.; Allison, S. A.; McCammon, J. A. Diffusion-Controlled Enzymatic Reactions. In *Methods in Enzymology*; Academic Press: New York, 1991; Vol. 202, pp 473–498.
(18) Smoluchowski, M. *Z. Phys. Chem.* **1917**, *92*, 129.
(19) Luty, B. A.; McCammon, J. A.; Zhou, H. X. *J. Chem. Phys.* **1992**, *97*, 5682.
(20) Wade, R. C.; Davis, M. E.; Luty, B. A.; Madura, J. D.; McCammon, J. A. *Biophys. J.*, in press.
(21) Brooks, B. R.; Bruccoleri, R. E.; Olafson, B. D.; States, D. J.; Swaminathan, S.; Karplus, M. *J. Comput. Chem.* **1983**, *4*, 187.
(22) Jorgensen, W. L.; Triado-Rives, J. *J. Am. Chem. Soc.* **1988**, *110*, 1657.
(23) Jarvis, L.; Huang, C.; Ferrin, T.; Langridge, R. UCSF MIDAS USER'S MANUAL, 1986.
(24) Edmonds, D. T.; Rogers, N. K.; Sternberg, M. J. E. *Molec. Phys.* **1984**, *52*, 1487–1494.
(25) Gilson, M. K.; Sharp, K. A.; Honig, B. H. *J. Comput. Chem.* **1987**, *9*, 327–335.
(26) Davis, M. E.; McCammon, J. A. *J. Comput. Chem.* **1989**, *10*, 386–391.
(27) Davis, M. E.; McCammon, J. A. *J. Comput. Chem.* **1991**, *12*, 909–912.
(28) Mathews, C. K.; van Holde, K. E. *Biochemistry*; Benjamin-Cummings: New York, 1990.
(29) Frisch, M. J.; Head-Gordon, M.; Trucks, G. W.; Foresman, J. B.; Schlegel, H. B.; Raghavachari, K.; Robb, M. A.; Binkley, J. S.; Gonzalez, C.; Defrees, D. J.; Fox, D. J.; Whiteside, R. A.; Seeger, R.; Melius, C. F.; Baker, J.; Martin, R. L.; Kahn, L. R.; Stewart, J. J. P.; Topiol, S.; Pople, J. A. *Gaussian90*; Gaussian, Inc.: Pittsburgh, PA, 1990.
(30) *Quanta v3.2*; Polygen/Molecular Simulations, Inc.: Waltham, MA, 1990.
(31) Lolis, E.; Petsko, G. A. *Biochemistry* **1990**, *29*, 6619–6625.
(32) Davis, M. E.; Madura, J. D.; Luty, B. A.; McCammon, J. A. *Comput. Phys. Commun.* **1991**, *62*, 187–197.
(33) Garcia de la Torre, J.; Bloomfield, V. A. *Biopolymers* **1977**, *16*, 1747–1763.
(34) Press, W. H.; Flannery, B. P.; Teukolsky, S. A.; Vetterling, W. T. *Numerical Recipes: The Art of Scientific Computing*; Cambridge University Press: Cambridge, 1986.